



BNL-27915

Search for Narrow States Produced in the Reaction
 $\pi^- p \rightarrow n + \text{neutrals}$ at 13 GeV/c

I-H. Chiang, R.A. Johnson, B. Kwan, T.F. Kycia, K.K. Li,
L.S. Littenberg, A. Wijangco, L.A. Garren, J.J. Thaler,
G.E. Hogan, K.T. McDonald and A.J.S. Smith

The submitted manuscript has been authored under contract DE-AC02-76CH00016 with the U.S. Department of Energy. Accordingly, the U.S. Government retains a nonexclusive, royalty-free license to publish or reproduce the published form of this contribution, or allow others to do so, for U.S. Government purposes.

Search for Narrow States Produced in the Reaction

$$\pi^- p \rightarrow n + \text{neutrals at } 13 \text{ GeV}/c$$

I-H. Chiang, R.A. Johnson, B. Kwan, T.F. Kycia, K.K. Li,

L.S. Littenberg and A. Wijangco

Brookhaven National Laboratory, Upton, New York 11973

L.A. Garren and J.J. Thaler

University of Illinois, Urbana, Illinois 61801

G.E. Hogan, K.T. McDonald and A.J.S. Smith

Princeton University, Princeton, New Jersey 08544

ABSTRACT

Using a double arm lead-glass lead-scintillator calorimeter system we have searched for narrow states, such as the η_c , produced in the exclusive reactions $\pi^- p \rightarrow \gamma\gamma n$, $\pi^- p \rightarrow \pi^0\gamma n$, and $\pi^- p \rightarrow \pi^0\pi^0 n$ at 13 GeV/c. We find a 90% c.l. upper limit $\sigma \cdot \text{BR} < 260 \text{ pb}$ for $\gamma\gamma$ states with masses from 2.2 to 4.0 GeV/c². Corresponding limits on narrow $\pi^0\gamma$ and $\pi^0\pi^0$ states are also given.

In the five years since the discovery of the J/ψ , many members of the charmonium family have been discovered, and, to a large extent, their masses and γ transition rates have been explained. This, together with the observed mass spectrum of explicitly charmed particles, has resulted in a rather coherent picture of the charmed quark spectroscopy. The major remaining mystery is the status of the 1S_0 states, η_c and η_c' . Early candidates from DESY⁽¹⁾ and SPEAR⁽²⁾ have recently been contradicted by the results of the Crystal Ball experiment.^(3,4)

An alternative approach to that of the storage rings is to attempt to produce the 1S_0 states via hadronic reactions. In such an experiment at 40 GeV/c, Apel et al.⁽⁵⁾ reported the observation of a narrow state X(2850) produced via $\pi p \rightarrow X^0 n$ and decaying into 2 γ 's. Experimental^(3,4) and theoretical⁽⁶⁾ developments since that work, however, indicate that this cannot be considered a viable candidate for the η_c , reopening the question of the nature of the object. In an attempt to confirm the X(2850), to throw light on its nature, and to search further for the η_c and η_c' , we have performed an experiment on the reaction $\pi\bar{p} \rightarrow X^0 n; X^0 \rightarrow \gamma\gamma, \pi^0\gamma, \pi^0\pi^0$ at 13 GeV/c.

The apparatus is indicated schematically in Fig. 1(a). A 13 GeV π^- beam derived from the Brookhaven AGS impinged on a longitudinally segmented scintillator target. Each of the six 2.87 cm diameter, 5.41 cm long cylindrical segments was viewed by its own photomultiplier tube allowing an accuracy of ± 2.5 cm in the determination of the interaction vertex. The target was surrounded on 4 sides by a layer of scintillator counter vetos, A. Used in conjunction with downstream vetos A0 and A2 these enforced the neutral final state (NFS) requirement.

A layer of 12 lead-scintillator shower counters, S, just outside the A counters were used to veto large angle γ 's from π^0 's. A set of 34 downstream lead-scintillator shower counters, V, operating as vetos, completed the aperture definition.

Within the aperture, photons were detected by two large 107 cm \times 213 cm photon calorimeters, 220" downstream of the target positioned symmetrically at $\pm 16^\circ$. One of these calorimeters is shown in Fig. 1(b). First came a converter section consisting of four radiation lengths of lead interspersed with scintillation counters. Each of two 1.3 r.l. layers of lead was followed by a plane of 15 cm wide scintillation counter strips. Light from each pair of aligned strips was added optically and brought to a single photomultiplier tube. Time of flight as well as pulse height information was recorded for these "calorimeter" counters. Next came an additional 1.3 radiation lengths of lead and two planes of scintillation counter hodoscopes: one vertical and one horizontal. In addition to augmenting the calorimetry measurements, these 2.54 cm wide "finger" counters located shower vertices to ± 6 mm. Following the converter section was a segmented lead glass calorimeter.⁽⁷⁾ The front lead glass wall consisted of a 15 \times 2 array of 15 cm wide \times 45 cm high \times 3 r.l. deep transversely mounted blocks. The rear wall was a 16 \times 7 array of 15 cm \times 15 cm \times 9 r.l. deep blocks. Each of the 648 detector elements was read out into a separate ADC channel. In addition, an analog energy sum was formed for each layer for triggering purposes. For long term calibration an Am²⁴¹ doped NaI source which provides a 5.5 MeV α line was glued to each lead glass counter, and Bi²⁰⁷ sources which emit conversion electrons at 0.975 and 1.050 MeV were glued to small scintillators visible to each photomultiplier tube in the converter section. Short term calibration was provided by a spark gap light flasher system which was fanned out via fiber optics to each pulse height measuring element.

Electron beams of energies between 2 and 10 GeV were diverted into the apparatus to provide an absolute calibration of the calorimeter elements. The fractional energy resolution achieved for electrons was $12\%/\sqrt{E}$ (E in GeV).

The normal trigger for the experiment was

$$\text{BEAM} \cdot \overline{S} \cdot \overline{V} \cdot (E_L > 1 \text{ GeV}) \cdot (E_R > 1 \text{ GeV}) \cdot (E_L + E_R > 9 \text{ GeV})$$

where $\text{BEAM} = B_1 \cdot B_2 \cdot \overline{B}_A$, NFS (neutral final state) = $\overline{A} \cdot \overline{A}_0 \cdot \overline{A}_2$, and E_L (E_R) is the analog energy sum for the left (right) arm. Simultaneous triggers were taken with $\text{BEAM} \cdot (E_L > 1 \text{ GeV}) \cdot (E_R > 1 \text{ GeV})$

$$\text{and } \text{BEAM} \cdot \overline{S} \cdot \overline{V} \cdot (E_L > 9 \text{ GeV or } E_R > 9 \text{ GeV})$$

for normalization and calibration purposes.

In addition, special runs were taken with the incident π^- beam momentum reduced to 6 GeV/c, and at 2, 4, 6, 8 and 10 GeV/c with the beam and target aligned with the center line of one spectrometer arm.

During normal running the beam intensity was $\sim 10^7/\text{burst}$. Altogether, approximately 2.4×10^6 triggers were recorded. For each event, all detector pulse heights were corrected for gain drift and attenuation, and corrected times of flight were calculated for calorimeter hits. The events were then subjected to a pattern recognition program which combined contiguous pulse height depositions into clusters, classified these clusters as one- or two-photon showers, and calculated their energies. Associating these with the vertex determined by the target counters allowed 4-momenta and effective masses to be calculated.

Figure 2(a) shows the $M_{\gamma\gamma}$ spectrum for events in which there are 2 separated γ clusters on a single arm. A clear π^0 peak is observed over a small background. The mean $M_{\gamma\gamma}$ is $133 \text{ MeV}/c^2$, indicating that the energy scale determined by the electron calibration is also correct for photons, while the rms width ($\sigma = 11.6 \text{ MeV}/c^2$) implies a fractional energy resolution of $15\%/\sqrt{E}$ for photons.⁸

The vast majority of triggers were $\pi^- p \rightarrow \pi^0 \pi^0 n$ events in which all four γ 's hit the active area of the detector, or in which one soft γ struck a veto counter but deposited less than the threshold energy setting.

We found that γ 's had a $\sim 95\%$ probability of making an identifiable shower in the finger counters. Since nearly all the energy of these showers was confined to 2 or 3 finger counters, and since the minimum opening distance for π^0 's in our experiment was ~ 6 finger counters, 90% of π^0 's in which both γ 's struck the detector could be immediately recognized. In cases where only one γ converted in the finger counters, the π^0 could be readily identified by the failure of the finger shower ($\sigma_{x,y} \sim 6$ mm) to line up with the lead glass shower ($\sigma_{x,y} \sim 12$ mm), and by the transverse extent of the shower in the lead glass. These yielded a further factor $\gtrsim 50$ in rejection so that only $\lesssim 0.2\%$ of π^0 's in which both γ 's struck the detector were mistaken for single γ 's. A more serious source of leak-through π^0 's was due to very asymmetric decays in which the low energy γ escaped the detector, either passing through the small beam exit aperture, or falling below the threshold of the veto it struck. Approximately 1.2% of π^0 's fall into this category. In addition to shower quality requirements, cuts were made in residual veto pulse heights, calorimeter timing, and event geometry. Figure 2(b) shows the distribution in measured energy for $\pi^0 \pi^0$ events passing these cuts. The clean peak near 13 GeV testifies to the effectiveness of the trigger and of the selection procedure. On the basis of this result, the visible energy of each event was required to be within ± 1.5 GeV of that of the beam. Events were then fit kinematically using the mass of the final state neutron as a constraint. This reduced the estimated error on the $\gamma\gamma$, $\pi\gamma$, and $\pi^0 \pi^0$ effective masses to ~ 48 MeV/c² at 2.8 GeV/c².⁽⁹⁾

After cuts on goodness of fit, the overall probability that a $\pi^- p \rightarrow \pi^0 \pi^0 n$ event be mistaken for a $\pi^- p \rightarrow \gamma\gamma n$ event was reduced to $< 1/5000$.

Figures 3(a-c) show the $M_{\pi^0\pi^0}$, $M_{\pi^0\gamma}$, and $M_{\gamma\gamma}$ plots respectively for the 13 GeV/c running. In each case the solid line indicates the shape of the calculated acceptance. The $\pi^0\pi^0$ distribution falls smoothly from the acceptance edge with no significant structure out to 3.8 GeV/c². The $\pi^0\gamma$ spectrum (Fig. 3(b)) which is qualitatively rather similar is also devoid of significant structure. This spectrum is in fact entirely consistent with the predicted $\pi^0\pi^0$ feed-down indicated by the dotted line in Fig. 3(b).

The $\gamma\gamma$ mass spectrum is given in Fig. 3(c). Only 27 events pass all cuts and none of these exceed 2.2 GeV/c². Again, the observed spectrum is consistent with the level expected from $\pi^0\pi^0$ feed-down. Clearly, at the present level of statistics there is no evidence for any narrow resonance.

To obtain cross-section limits, the data of Figure 3 are corrected for acceptance, shower recognition efficiency, random vetos, beam attenuation in the target, neutron mass cut, and computer dead time. Figure 4 shows these extracted limits.⁽¹⁰⁾

Note that the 90% c.l. upper limit on $\sigma \cdot \text{BR}$ for $M_{\gamma\gamma} = 2.85 \text{ GeV}/c^2$ is 260 pb. This is to be compared with the 200 pb signal claimed by Apel et al.⁽⁵⁾ in their 40 GeV/c experiment. The process $\pi^- p \rightarrow \eta_c n$ is expected to proceed mainly via A_2 exchange as do $\pi^- p \rightarrow \eta n$ and $\pi^- p \rightarrow \eta' n$. The cross-section would be expected to scale⁽¹¹⁾ as p^{-1} to -1.5 , ignoring possible threshold effects. Thus 200 pb at 40 GeV/c would imply 600 - 1000 pb at 13 GeV/c (5.5-9 events), which is in clear disagreement with our result. If the X(2.85) were a 4-quark object as hypothesized by Lipkin et al.⁽¹²⁾ the cross section would be expected to go as $p^{-2.5}$.⁽¹⁰⁾ This leads to $\sigma \cdot \text{BR} = 3.3 \text{ nb}$ (31 events) at 13 GeV/c in even worse disagreement with our result.

We gratefully acknowledge the contributions of A.M. Halling to the data analysis.

This work was supported in part by the U.S. Department of Energy under Contract Nos. DE-AC02-76CH00016, DE-AC02-76ER01195 and DE-AC02-76ER03072.

References

- 1) W. Braunschweig et al., Phys. Lett. 67B, 1243 (1977).
- 2) J.S. Whitaker et al., Phys. Rev. Lett. 37, 1596 (1976).
- 3) R. Partridge et al., Phys. Rev. Lett. 44, 712 (1980).
- 4) E. Bloom SLAC-PUB-2425 (1979).
- 5) Apel et al., Phys. Lett. 72B, 500 (1978).
- 6) A.Yu. Khodjamirian E ϕ - 281 (6) - 78 (Yerevan Physics Institute preprint).
- 7) A.S. Carroll, et al, (submitted to Nucl. Inst. and Methods).
- 8) η , ω , η' , and f^0 peaks observed in the 6 GeV/c and single arm runs served to further verify both the energy scale and resolution indicated here.
- 9) The effective mass resolution varied from 30 MeV/c² at 1.8 GeV/c² to 95 MeV/c² at 3.8 GeV/c².
- 10) To extract these limits, isotopic decay and a t-distribution similar to that obtaining in $\pi^- p \rightarrow \eta' n$ were assumed.
- 11) G. Eilam, B. Margolis and S. Rudaz, Phys. Lett. 80B, 306 (1979).
- 12) H.J. Lipkin, H.R. Rubinstein and N. Isgur, Phys. Lett. 78B, 295 (1978).

Figure Captions

1. a) Experimental layout. S and V counters are lead scintillator shower counters. A are charged particle veto counters which surround the scintillator target.
b) Detail of one photon calorimeter. Components of the converter section are shown in an exploded view for clarity.
2. a) Single arm $M_{\gamma\gamma}$ spectrum
b) $E_{\pi^0\pi^0}$ spectrum.
3. Mass plots from normal runs. Solid curves indicate the acceptances. Dotted lines in (b) and (c) indicate the calculated $\pi^0\pi^0$ feed-down.
a) $\pi^0\pi^0$
b) $\pi^0\gamma$
c) $\gamma\gamma$
4. 90% c.l. limits for narrow resonance production for $\pi^0\pi^0$, $\pi^0\gamma$, and $\gamma\gamma$.

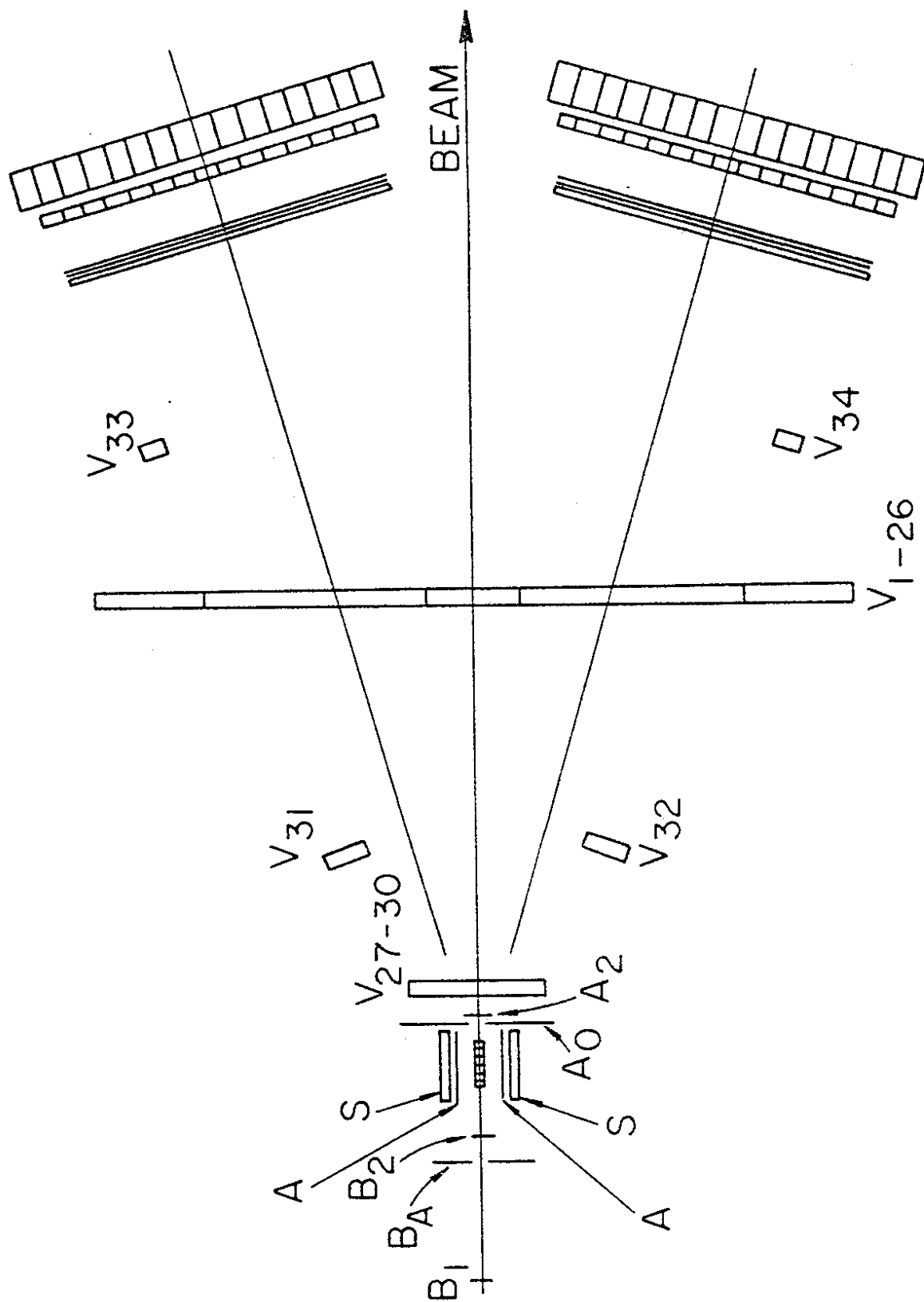


Fig. 1(a)

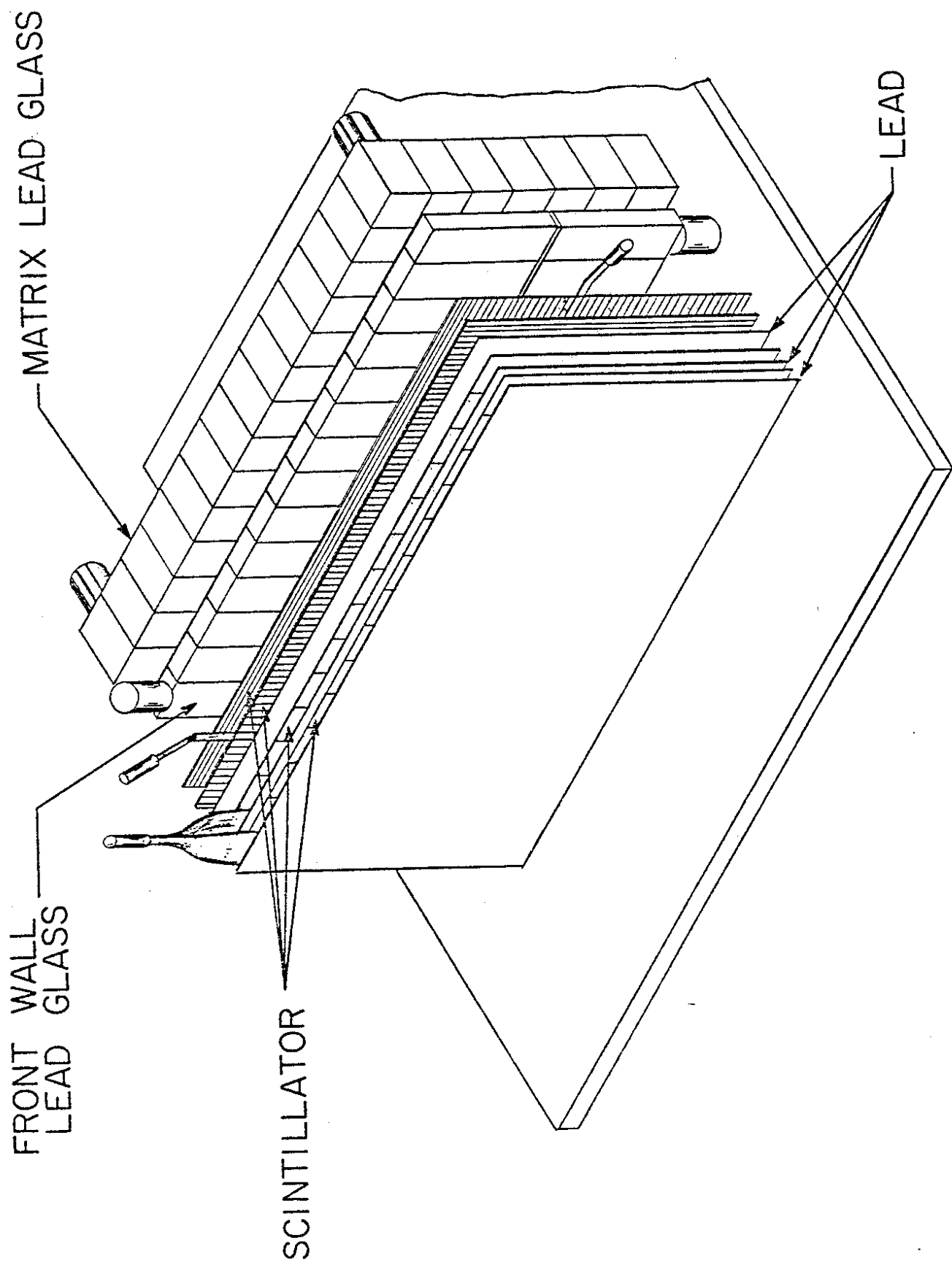


Fig. 1(b)

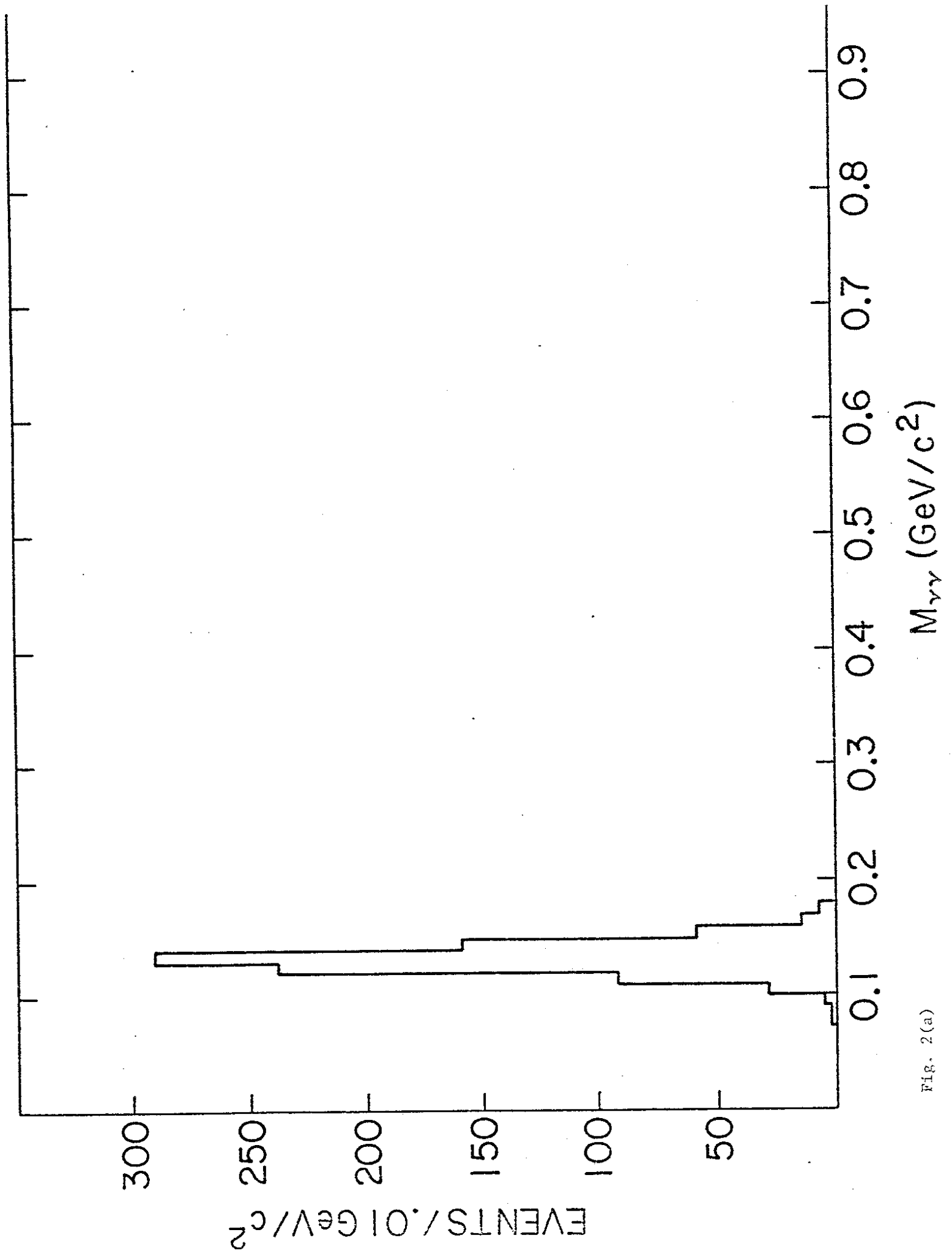


Fig. 2 (a)

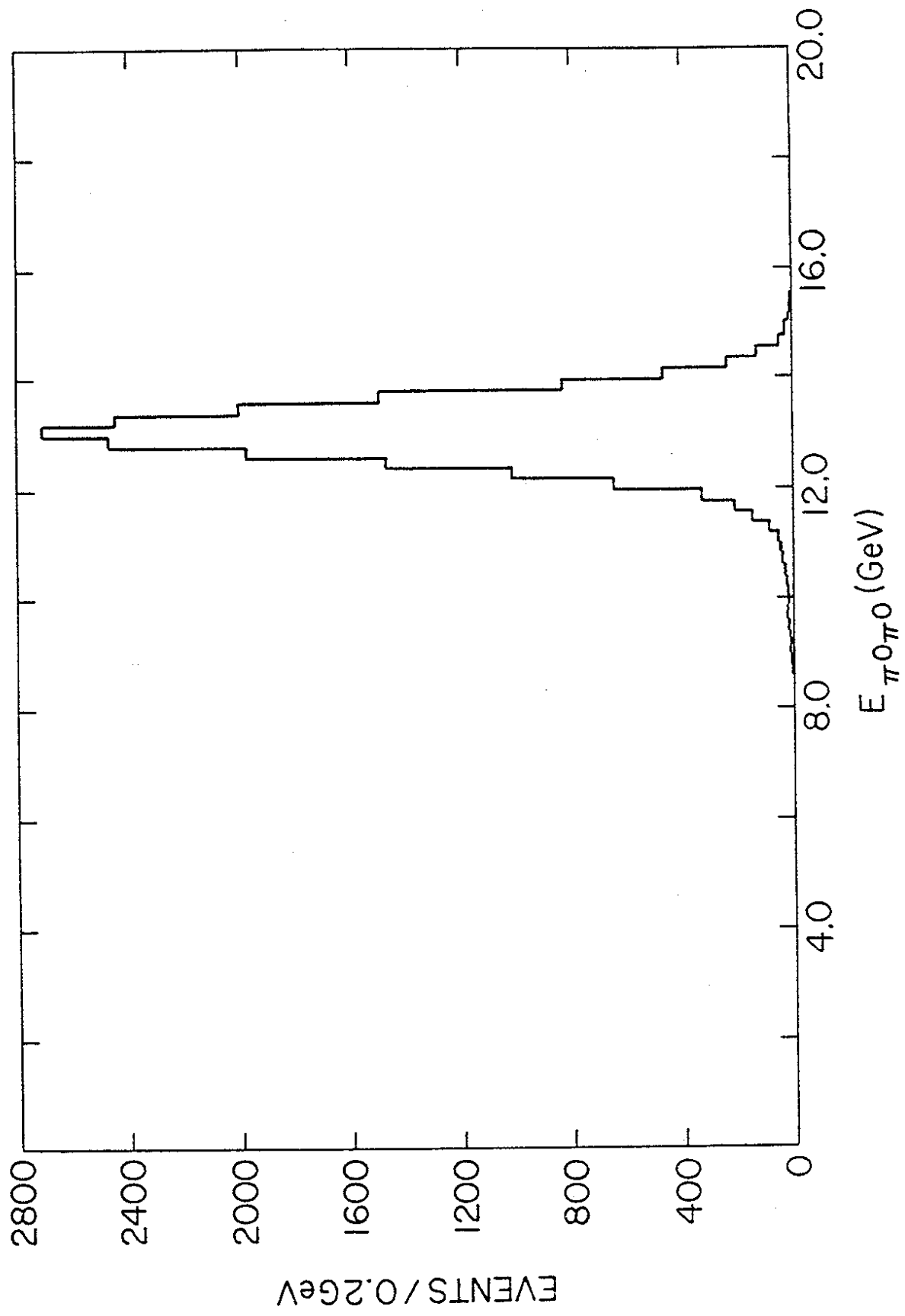


Fig. 2 (b)

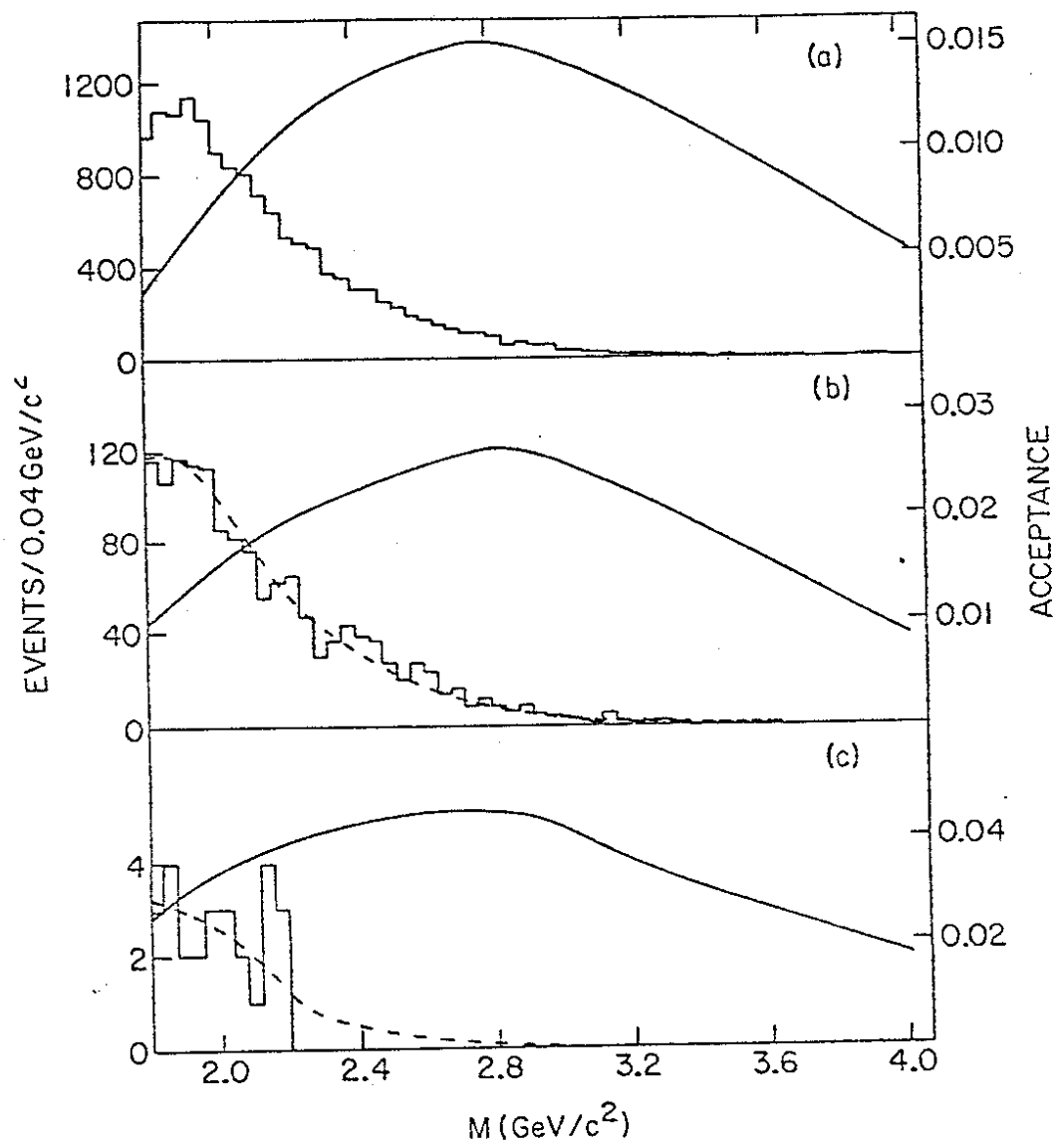


Fig. 3

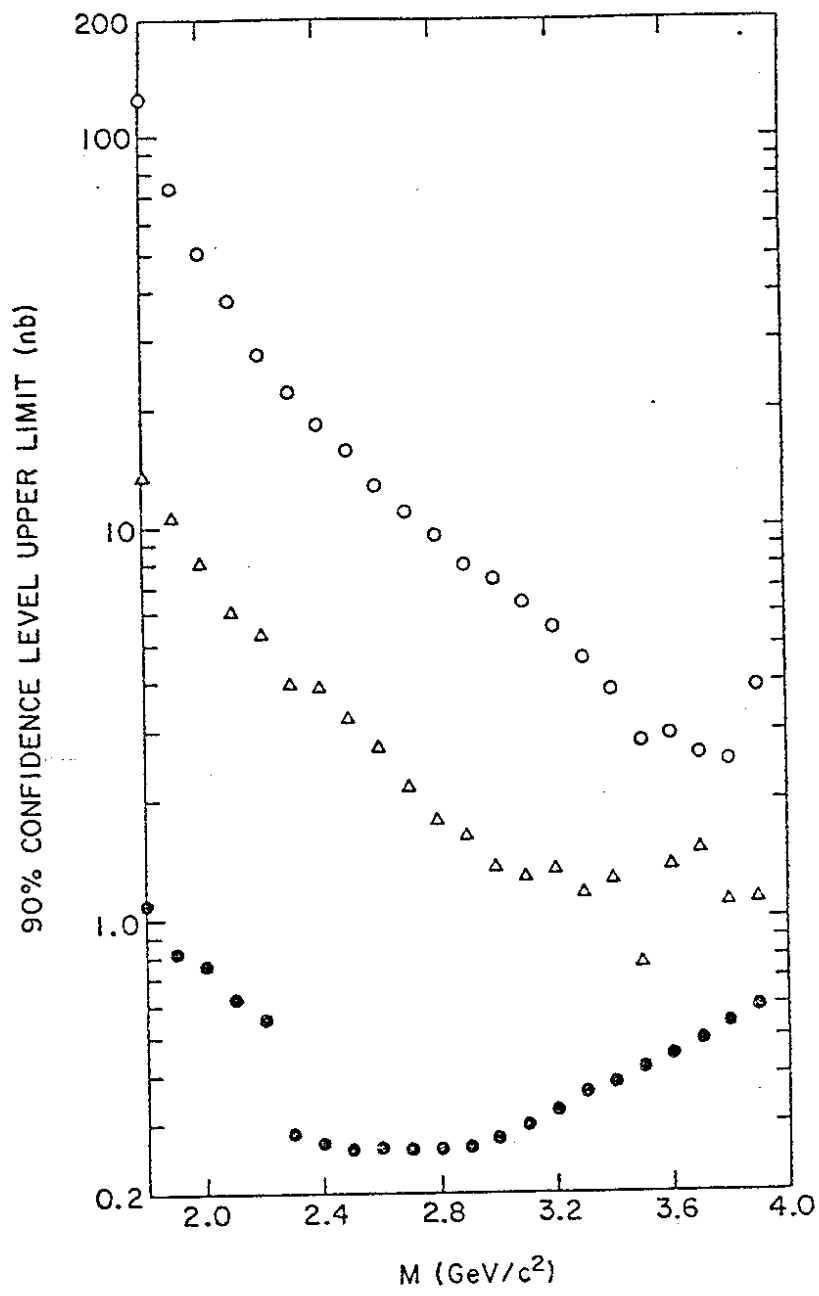


Fig. 4